Supplemental material

I. NUMERICAL CALCULATIONS

All event samples (NP signal and SM background) were generated using MadGraph5_aMC@NLO [1] at LO parton-level and with the SMEFTsim model of [2, 3] for the EFT framework. The 5-flavor scheme was used to generate all samples, with the `NNPDF30_lo_as_0130` PDF set [4] and the default MadGraph5_aMC@NLO LO dynamical scale.

Both the NP and the SM tri-lepton production cross-sections were calculated with an additional jet. In particular, for the NP: $pp \to t(\bar{t})\ell^+\ell^-$ and $pp \to t(\bar{t})\ell^+\ell^- + j$ followed by the top(anti-top) decay $t(\bar{t}) \to b\ell'^+\nu_{\ell'}(\bar{b}\ell'^-\bar{\nu}_{\ell'})$, while for the SM: $pp \to ZW^\pm$ and $pp \to ZW^\pm + j$ followed by $Z \to \ell^+\ell^-$ and $W^\pm \to \ell'^\pm\nu_{\ell'}$.

Leptons were required to have transverse momentum of $p_{\rm T} > 10$ GeV and pseudo-rapidity $|\eta| < 2.5$, while for jets we used $p_{\rm T} > 20$ GeV, $|\eta| < 5.0$ and an angular separation of $\Delta R = 0.4$.

In Table I we list the estimated cross-sections for the NP with $\Lambda = 1$ TeV (note that the NP cross-section scales as Λ^{-4}) and the SM contributions to the inclusive $pp \to \ell'^\pm\ell^+\ell^- + X$ processes for $m_{min}(\ell^+\ell^-) = 200$, 300 and 400 GeV, where $m_{min}(\ell^+\ell^-)$ is the lower cut on the invariant mass of the same-flavor di-leptons. In particular, the $m_{min}(\ell^+\ell^-)$-dependent cross-sections are defined as:

$$\sigma_{m_{min}(\ell^+\ell^-)} \equiv \int_{m(\ell\ell)\geq m_{min}(\ell^+\ell^-)} dm(\ell\ell)\frac{d\sigma}{dm(\ell\ell)} \ . \quad (1)$$

We note that the simulations were made without parton showering and jet matching, which has no effect on our CP-asymmetry (we confirmed that the calculated CP-asymmetry with and without the extra jet in the tri-lepton final state is the same within the numerical error). Also, we did not perform any detector simulation which is beyond the scope of this work and is left for a dedicated analysis. Thus, the cross-sections reported in Table I should be viewed as an estimate; a more realistic calculation of the expected total cross-sections for this type of NP and SM background can be found in [5].

II. DEPENDENCE OF THE CP-ASYMMETRY ON THE NP SCALE

In Fig.1 we show the dependence of A_{CP} on the NP scale Λ, with parameters as indicated in the caption of the figure. We see that the asymmetry in the ug-fusion case falls rather slowly in the range $\Lambda \sim 1 - 4$ TeV, whereas in the cg-fusion case it drops steeply in this range, approaching $1/\Lambda^4$ where the SM contribution to the inclusive tri-lepton background dominates.

TABLE I: The estimated cross-sections in [fb], for the NP tri-lepton signals and the SM tri-lepton background. Values are given for the NP parameters $\mathrm{Im}\,(f_S f_T^\star) = 0.25$, $\Lambda = 1$ TeV and for three values of $m_{min}(\ell^+\ell^-)$ as indicated. Also, all acceptance cuts (e.g., p_T and η of the leptons) have been applied, see also description in the text.

$m_{min}(\ell^+\ell^-)[GeV] \Rightarrow$	200	300	400
$\sigma_{NP}(pp_{ug} \to \ell'^-\ell^+\ell^- + X)$	12.43	11.65	10.84
$\sigma_{NP}(pp_{\bar{u}g} \to \ell'^+\ell^-\ell^+ + X)$	0.98	0.87	0.76
$\sigma_{NP}(pp_{cg} \to \ell'^-\ell^+\ell^- + X)$	0.37	0.32	0.27
$\sigma_{NP}(pp_{\bar{c}g} \to \ell'^+\ell^-\ell^+ + X)$	0.37	0.32	0.27
$\sigma_{SM}(pp \to \ell'^-\ell^+\ell^- + X)$	0.33	0.11	0.05
$\sigma_{SM}(pp \to \ell'^+\ell^-\ell^+ + X)$	0.56	0.21	0.10

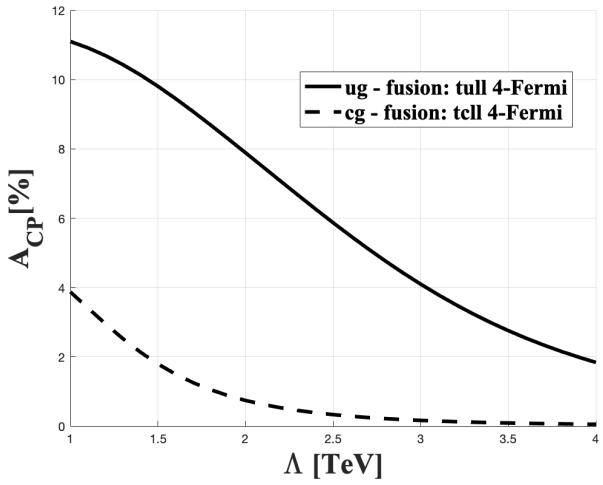

FIG. 1: The expected CP-asymmetry A_{CP}, as a function of the NP scale Λ, for $m_{min}(\ell^+\ell^-) = 400$ GeV and $\mathrm{Im}\,(f_S f_T^\star) = 0.25$. Results are shown for the cases of NP from ug and cg-fusion, which arise from the $tu\ell\ell$ and $tc\ell\ell$ 4-Fermi operators, respectively. The SM background is calculated from $pp \to ZW^\pm + X$.

TABLE II: The expected T_N-odd and CP asymmetries A_T, $\bar{A}_T$, A_{CP} and the corresponding axis-dependent asymmetries A_T^i, $\bar{A}_T^i$, A_{CP}^i $(i = x, y, z)$, for the tri-lepton events $pp \to \ell'^{\pm}\ell^+\ell^- + X$ at the LHC with $m_{min}(\ell^+\ell^-) = 400$ GeV. Results are given for both the ug-fusion and cg-fusion production channels (and the CC ones). Numbers are presented for $\Lambda = 1$ TeV, $\mathrm{Im}\,(f_S f_T^\star) = 0.25$ and the dominant SM background from $pp \to ZW^\pm + X$ is included. The cases where an asymmetry is $\lesssim 0.5\%$ is marked by an X.

	A_{CP}	A_{CP}^x	A_{CP}^y	A_{CP}^z
ug-fusion:	11.1%	8.1%,	8.1%	X
cg-fusion:	3.9%	X	X	5.6%

	A_T	A_T^x	A_T^y	A_T^z
ug-fusion:	16.4%	11.3%,	10.7%	3.8%
cg-fusion:	3.1%	5.0	X	X

	$\bar{A}_T$	$\bar{A}_T^x$	$\bar{A}_T^y$	$\bar{A}_T^z$
ug-fusion:	-5.8%	-5.0%	-5.6%	3.1%
cg-fusion:	-4.7%	-6.3%	X	X

III. AXIS-DEPENDENT CP-VIOLATING TRIPLE PRODUCT OBSERVABLES

The triple products considered in the paper:[1]

$$\mathcal{O}_{\mathtt{CP}} = \vec{p}_a \cdot (\vec{p}_b \times \vec{p}_c) \ , \tag{2}$$

can be divided into three axis-sensitive triple-products:

$$\mathcal{O}_{\mathtt{CP}}^i = p_a^i \cdot (\vec{p}_b \times \vec{p}_c)^i \ , \tag{3}$$

where $i = x, y, z$ denotes the x, y, z components of the momenta, e.g., p_a^z and $(\vec{p}_b \times \vec{p}_c)^z$ are the z-components of the momenta $\vec{p}_a$ and $(\vec{p}_b \times \vec{p}_c)$, respectively. Note that only three out of the four $\mathcal{O}_{\mathtt{CP}}$ and $\mathcal{O}_{\mathtt{CP}}^{x,y,z}$ in (2) and (3) are independent, since $\mathcal{O}_{\mathtt{CP}} = \sum_{i=x,y,z} \mathcal{O}_{\mathtt{CP}}^i$. Furthermore, the axis-sensitive $\mathcal{O}_{\mathtt{CP}}^{x,y,z}$ transform under P,C,CP and T_N the same as $\mathcal{O}_{\mathtt{CP}}$, so that all the discussion and formulae for $\mathcal{O}_{\mathtt{CP}}$ in the paper applies also to $\mathcal{O}_{\mathtt{CP}}^{x,y,z}$. In particular, the axis-dependent CP-asymmetries can be similarly defined as:

$$A_{CP}^{x,y,z} = \frac{1}{2}\left(A_T^{x,y,z} - \bar{A}_T^{x,y,z}\right) \ , \tag{4}$$

where $A_T^{x,y,z}$ and $\bar{A}_T^{x,y,z}$ are the axis-dependent T_N-odd asymmetries.

In Table II we show a sample of our results for all T_N-odd and CP-asymmetries including the axis dependent ones, for the tri-lepton events $pp \to \ell'^{\pm}\ell^+\ell^- + X$ at the LHC, which are considered in this paper. The asymmetries are calculated for both the ug-fusion and cg-fusion production channels (and the CC ones), with $m_{min}(\ell^+\ell^-) = 400$ GeV , $\Lambda = 1$ TeV and $\mathrm{Im}\,(f_S f_T^\star) = 0.25$, and the dominant SM background from $pp \to ZW^\pm + X$ is considered. We see that a measurement of the axis-dependent asymmetries can be used to distinguish between the $tu\ell\ell$ and the $tc\ell\ell$ CP-violating dynamics. In particular, in the $tu\ell\ell$ case we obtain $A_{CP}^z \to 0$ and $A_{CP}^{x,y} \sim 8\%$, while for the $tc\ell\ell$ operator we find $A_{CP}^z \sim 5.5\%$ and $A_{CP}^{x,y} \to 0$. Note also that the axis-dependent asymmetries may yield a larger effect, e.g., in the cg-fusion case we find that $A_{CP}^z > A_{CP}$.

IV. DIFFERENTIAL DISTRIBUTIONS: SIGNAL VS. BACKGROUND

In Figs. 2 and 3, we plot the di-muon invariant mass and the triple-product differential distributions, respectively, for an integrated luminosity of $\mathcal{L} = 1000$ fb^{-1}. We show these distributions for the ug-fusion and the CC $\bar{u}g$-fusion NP cases and the corresponding SM backgrounds, assuming a NP scale of $\Lambda = 1$ TeV and/or $\Lambda = 2$ TeV. Note that the NP signals scale as Λ^{-4} and are calculated with our benchmark value for the CPV coupling $\mathrm{Im}\,(f_S f_T^\star) = 0.25$. Also, the triple-product distributions in Fig. 3 are calculated with $m_{min}(\ell^+\ell^-) = 300$ GeV.

[1] Johan Alwall, Michel Herquet, Fabio Maltoni, Olivier Mattelaer, and Tim Stelzer. MadGraph 5 : Going Beyond. *JHEP*, 06:128, 2011, 1106.0522.

[2] Ilaria Brivio, Yun Jiang, and Michael Trott. The SMEFTsim package, theory and tools. *JHEP*, 12:070, 2017, 1709.06492.

[3] Ilaria Brivio. SMEFTsim 3.0 — a practical guide. *JHEP*, 04:073, 2021, 2012.11343.

[4] Richard D. Ball et al. Parton distributions for the LHC Run II. *JHEP*, 04:040, 2015, 1410.8849.

[5] Yoav Afik, Shaouly Bar-Shalom, Amarjit Soni, and Jose Wudka. New flavor physics in di- and trilepton events from single-top production at the LHC and beyond. *Phys. Rev. D*, 103(7):075031, 2021, 2101.05286.

[1] The triple products are defined in the laboratory frame and we expect that systematic uncertainties in the reconstruction of the momenta involved will be smaller then e.g., the case where the momenta are defined in a rest frame of some particle(s). Also, the kinematical cuts on the leptons involved should be CP-symmetric, e.g., same p_T cuts should be applied to all leptons.

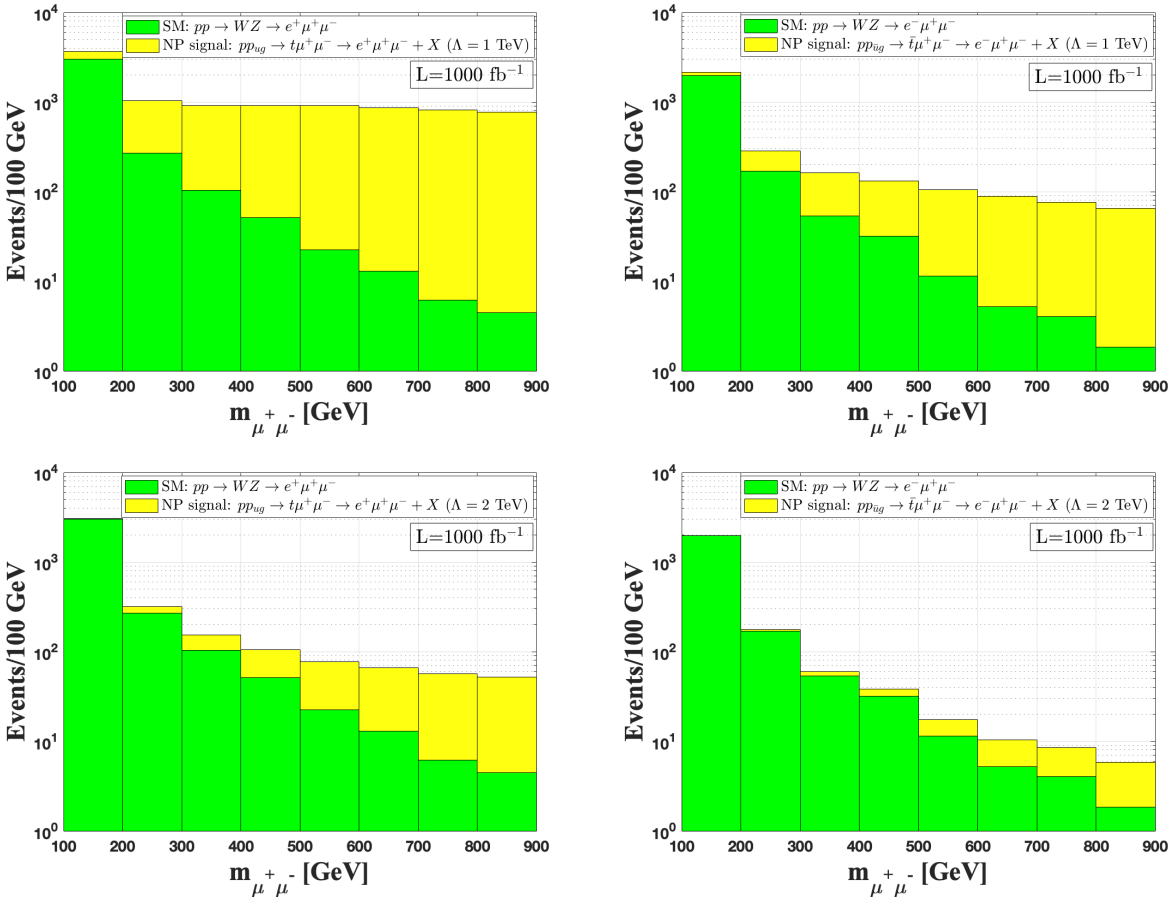

FIG. 2: Di-muon invariant mass distribution (stacked) for the tri-lepton $e^+\mu^+\mu^-$ (left figures) and $e^-\mu^+\mu^-$ (right figures) signals, from ug-fusion and $\bar{u}g$-fusion NP processes, respectively, and the corresponding SM backgrounds. The distributions are shown per integrated luminosity of $\mathcal{L} = 1000$ fb^{-1}, for $\Lambda = 1$ TeV (upper figures) and $\Lambda = 2$ TeV (lower figures).

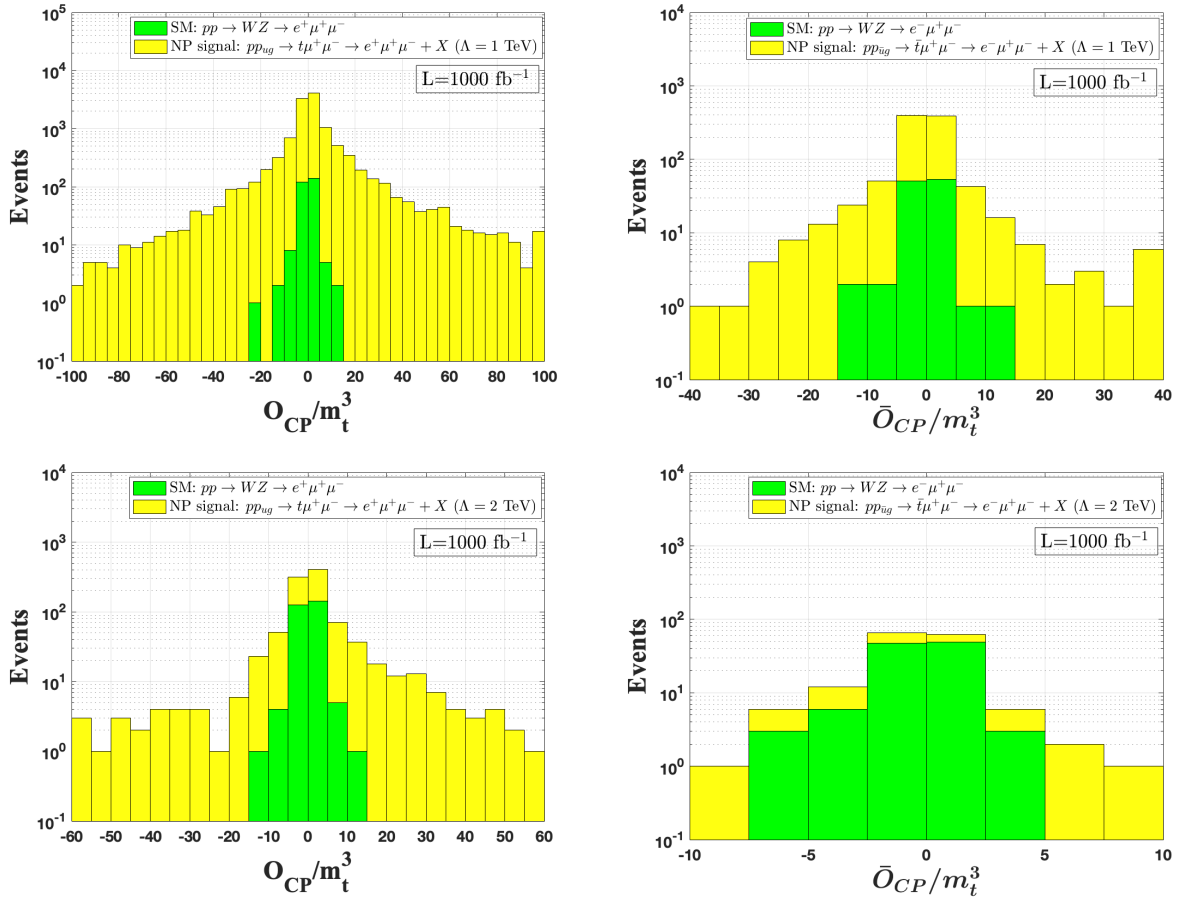

FIG. 3: Differential distribution (stacked) of the triple products $\mathcal{O}_{CP}$ (left figures) and $\bar{\mathcal{O}}_{CP}$ (right figures) in the tri-lepton NP signals and corresponding backgrounds. The NP is from $ug \to t\mu^+\mu^- \to e^+\mu^+\mu^-$ (left figures) and $\bar{u}g \to \bar{t}\mu^+\mu^- \to e^-\mu^+\mu^-$ (right figures) with $\Lambda = 1$ TeV (upper figures) and $\Lambda = 2$ TeV (lower figures). The distributions for both signal and background are calculated with the cut on the di-muon invariant mass of $m_{min}(\ell^+\ell^-) = 300$ GeV and per integrated luminosity of $\mathcal{L} = 1000$ fb^{-1}. See also text.